Spin Purification in Full-CI Quantum Monte Carlo via a First-Order Penalty Approach

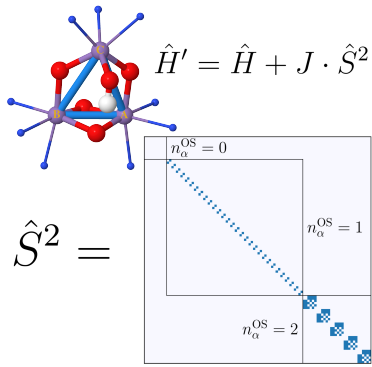Oskar Weser,[*,†] Niklas Liebermann,[†] Daniel Kats,[†] Ali Alavi,[†,‡] and Giovanni Li Manni[*,†]

†*Max-Planck-Institute for Solid State Research, Stuttgart, Germany*

‡*Dept of Chemistry, University of Cambridge, Lensfield Road, Cambridge CB2 1EW, United Kingdom*

E-mail: oskar.weser@gmail.com; g.limanni@fkf.mpg.de

Abstract: In this Letter we demonstrate that a first-order spin penalty scheme can be efficiently applied to the Slater determinant based Full-CI Quantum Monte-Carlo (FCIQMC) algorithm, as a practical route towards spin purification. Two crucial applications are presented to demonstrate the validity and robustness of this scheme; the $^1\Delta_g \leftarrow {}^3\Sigma_g$ vertical excitation in O_2, and key spin gaps in a $[Mn_3O_4]^{3+}$ cluster. In the absence of a robust spin adaptation/purification technique, both applications would be unattainable by Slater determinant based ground state methods, with any starting wave function collapsing into the higher-spin ground state during the optimization. This strategy can be coupled to other algorithms that use FCIQMC as configuration interaction eigensolver, including the Stochastic Generalized Active Space, the similarity-transformed FCIQMC and second-order perturbation theory approaches. Moreover, in contrast to the GUGA-FCIQMC technique, this strategy features both spin projection and total spin adaptation, making it appealing when solving anisotropic Hamiltonians.

TOC Graphic

Strongly open-shell molecules present a number of challenges to quantum chemical methods, arising from the large number of nearly degenerate states with different total spin quantum number, S, which exist in such systems and are in general hard to resolve. In these systems spin contamination is a major problem for an accurate description of their electronic spectrum. Such systems usually exhibit a strong *multi-reference* character, with numerous dominant electronic configurations featuring similar weights in the configuration interaction (CI) expansion. Furthermore, when a high-spin state is the ground-state, states of the same symmetry but with lower spin are impossible to obtain with ground state projective techniques. For these reasons, there has been much interest in recent years in developing spin-adapted approaches, which work in Hilbert spaces of *configuration state functions* (CSFs), rather than Slater determinants (SDs).[1–16] In these approaches, $\hat{S}^2$ symmetry is explicitly enforced, ensuring zero spin contamination, and enabling the targeting of any desired spin state. The Graphical Unitary group approach (GUGA)[17–26] is one such example of a fully spin-adapted approach, which we have implemented within the stochastic full-CI quantum monte carlo (FCIQMC)[9,27?–30] and the Stochastic-CASSCF[10,31,32] frameworks. Recently, we have discovered a strategy within GUGA, that allows an unprecedented reduction of the multi-reference character (compression)[32–35] and the unique possibility to perform state-specific optimizations of ground- and excited-state wave functions.[34,35] These properties arise from a unique block-diagonal structure of the GUGA Hamiltonian matrix even within the same spin-symmetry sector, that follow chemically/physically motivated molecular orbital transformations.[34] This strategy has been applied to exchange-coupled polynuclear transition metal clusters with a large number of localized open-shell orbitals,[32–35] and to one-dimensional Heisenberg and Hubbard model Hamiltonians.[36] Other sparse FCI solvers[2,37–48] could also benefit from the enhanced sparsity of the Hamiltonian and wave functions that follow the above mentioned strategy.

On the other hand, such sophisticated approaches to spin-adaptation incur a number of complications related to their increased algorithmic complexity, including matrix element calculation and excitation generation process.[9,32] Furthermore, more compli-

cated Hamiltonians (including anisotropic spin, or three-body interactions) cannot be easily accommodated, and in systems with a more delocalized character (i.e. covalency), the aforementioned compression advantages of the GUGA method are less evident. For these reasons, it is highly desirable to have a Slater determinant-based approach to spin-adaptation, which is possible via *spin-purification* concepts.

For cases with an even number of unpaired electrons, such as the oxygen dimer discussed later, it is also possible to place constraints on the spin by applying time-reversal symmetry and by working with pairs of spin-coupled functions.[49] This reduces the size of the Hilbert space by a factor of two, while reducing any spin-contamination, as in the reduced space either all even or odd spin states can be excluded. However, this strategy cannot separate singlet from quintet, nor can it operate in cases with an odd number of unpaired electrons.

The aim of the present Letter is to introduce one such method, based on a simple first-order spin-penalty approach, within the context of Slater-determinant based FCIQMC. Spin purification techniques, including the first-order spin penalty approach, have recently been discussed in details by Levine and co-workers[50] and have already been utilized in the context of renormalization approaches.[51,52] We build on the existing literature by explaining the origin for an optimal spin penalty parameter.

We write the total spin operator, $\hat{S}^2$, in terms of the spin projection, $\hat{S}_z$, and the ladder operators, $\hat{S}_+$ (raising) and $\hat{S}_-$ (lowering) (see also ref 53), namely

$$\hat{S}^2 = \hat{S}_z(\hat{S}_z - 1) + \hat{S}_+\hat{S}_- \quad . \tag{1}$$

Given two SDs, $|D_i\rangle$ and $|D_j\rangle$, the expression for $\langle D_i|\hat{S}^2|D_j\rangle$ is then given by

$$\langle D_i|\hat{S}^2|D_j\rangle = \begin{cases} \hat{S}_z(\hat{S}_z - 1) + n_\alpha^{\mathrm{OS}} & |D_i\rangle = |D_j\rangle \text{ (Diagonal elements)} \\ \mathrm{sgn}(D_i, D_j) & |D_j\rangle = \hat{a}_{p\alpha}^\dagger \hat{a}_{p\beta} \hat{a}_{q\beta}^\dagger \hat{a}_{q\alpha}|D_i\rangle, \ p \neq q \\ 0 & \text{else} \end{cases} \tag{2}$$

where n_α^{OS} is the number of unpaired (open-shell, OS) α electrons. The off-diagonal el-

4

ements are non-zero only for exchange excitations and are equal to $\text{sgn}(D_i, D_j) = \pm 1$, where the sign is given by the product of fermionic phase factors.[53] Since exchange excitations require the same orbital configuration in both determinants, the $\hat{S}^2$ matrix features an interesting block diagonal structure. Larger blocks are characterized by a common n_α^{OS} value, while the sub-blocks are characterized by a common occupation number vector. This block-diagonal and sparse structure (see Figure 1) is particularly well suited for FCIQMC.
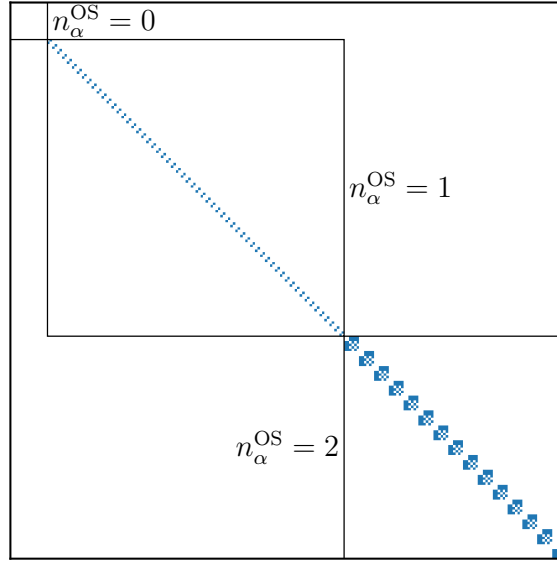

Figure 1: Block-diagonal structure of the $\hat{S}^2$ matrix in the SD basis of an (8,6) active space with $S_z = 0$, corresponding to a minimum active space for the singlet state of oxygen. White denotes zero, while blue denotes ± 1 entries. The diagonal is omitted.

In the first-order spin penalty approach a modified Hamiltonian

$$\hat{H}' = \hat{H} + J \cdot \hat{S}^2, \quad 0 < J \in \mathbb{R} \tag{3}$$

is utilized. If J is chosen such that the low-spin state becomes the lowest state in the modified $\hat{H}'$ Hamiltonian, ground state methods, including FCIQMC, will converge to that state. The on-the-fly evaluation of modified Hamiltonian matrix elements does not require additional memory and has negligible runtime costs for the evaluation of the $\hat{S}^2$ correction. Since $\hat{H}$ and $\hat{S}^2$ commute, the eigenstates of $\hat{H}'$ are still eigenstates of $\hat{H}$ and the eigenvalues of $\hat{H}$ can be directly calculated from the corresponding eigenvalues

of $\hat{H}'$ by subtracting $J \cdot S(S+1)$. Note that this subtraction can be performed only for converged eigensolutions in a well-defined manner. For unconverged, intermediate results, for example along FCIQMC dynamics and before stationary conditions are reached, it is necessary to evaluate directly the original Hamiltonian $\hat{H}$. In the present work we calculate the latter as an expectation value from the stochastically sampled one- and two-body reduced density matrices (RDMs).

For the unique *critical* J value that makes the low- and high-spin states degenerate (*flipping point*), a spin-symmetry-broken wave function is to be expected, which is an arbitrary admixture of the degenerate spin states in the modified Hamiltonian. This *flipping point* satisfies the following relation

$$J_{\mathrm{f}} = -\frac{\Delta E_{\mathrm{m}}}{\Delta \langle \hat{S}^2 \rangle} \quad , \tag{4}$$

where the generally unknown value $\Delta E_{\mathrm{m}} = E_{\mathrm{hs}} - E_{\mathrm{ls}}$ corresponds to the energy gap between the high-spin (hs) and the desired low-spin (ls) state, and $\Delta \langle \hat{S}^2 \rangle = S_{\mathrm{hs}}(S_{\mathrm{hs}} + 1) - S_{\mathrm{ls}}(S_{\mathrm{ls}} + 1)$. For J values larger than the flipping point the desired low-spin state is obtained in the long-time limit. However, the speed of convergence and stability of the imaginary-time propagation in FCIQMC depends on how far J is from the flipping point.

At first glance one could expect that, above the flipping point, higher J values only improve the speed of convergence, because they increase the energy of the high-spin state, so an imaginary-time propagation with the modified Hamiltonian $\exp\left(-\tau(\hat{H}' - E_0)\right)$ projects out the high-spin state faster. But, as we (*vide infra*) and Levine et al.[50] observed, there is an optimal J value, and the convergence deteriorates upon further increasing it. This property arises, because for larger J values the modified Hamiltonian can be interpreted as mainly a $\hat{S}^2$ operator, corrected by a small perturbation represented by $\hat{H}$. Diagonalization of the pure $\hat{S}^2$ operator results in numerous degenerate eigenstates with equivalent spin eigenvalues (not energies), the lowest being $S(S+1) = 0$ or $S(S+1) = \frac{3}{4}$ for even and odd numbers of electrons, respectively. This degeneracy is in part lifted by the Hamiltonian $\hat{H}$. For very large J values the $\hat{H}$ correction becomes relatively smaller and projecting out the high-energy states of same spin harder.

The robustness of the spin penalty method in SD-based FCIQMC has been investigated in two crucial test-case applications. We investigated the vertical $^1\Delta_g \leftarrow {}^3\Sigma_g$ transition in the O_2 molecule using a full-CI expansion in a double-ζ quality basis set, and the vertical $\Gamma^{(1/2)} \leftarrow \Gamma^{(3/2)}$ (and $\Gamma^{(9/2)}$) transition in a $[Mn_3O_4]^{3+}$ tri-nuclear cluster. In both cases the ground state is the higher spin-state.

Oxygen dimer. We used a distance of $1.203\,\text{Å}$, and correlated 16 electrons in the 28 orbitals of an ANO-RCC-VDZP basis.[54,55] The Full-CI calculations were performed on the basis of the state-specific CASSCF(8,6) orbitals. A spin-pure calculation using GUGA-FCIQMC served as reference. The J parameter was set to $0.12\,E_\text{h}$.

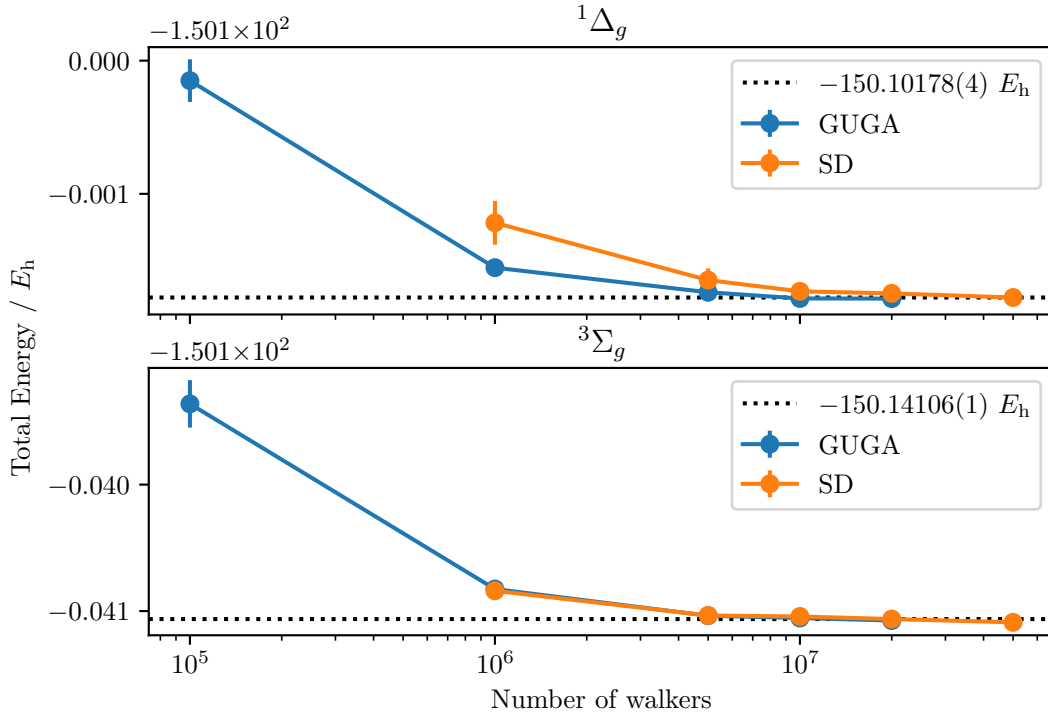The $\langle \hat{H} \rangle$ expectation value calculated from RDMs is shown in Figure 2. The triplet

Figure 2: Total energy calculated from RDMs for the $^1\Delta_g$ (upper plot) and the $^3\Sigma_g$ (lower plot) spin states of the oxygen molecule.

converges faster than the singlet and its total energy nearly matches the energy of the GUGA reference calculation for the same walker number. Generally, convergence with respect to the number of walkers in initiator-FCIQMC is mainly influenced by the compactness of the respective wave function. The triplet calculation started from a SD with

$|M_S| = 1$, which is also the spin-pure configuration that dominates the FCI wave function for this electronic state. On the contrary, in the case of the singlet spin state, a multi-determinantal wave function is required to correctly describe the spin-pure reference space, therefore the calculation converges slower with respect to walker number than the GUGA-based one. However, the wall clock time to achieve the same quality of convergence is roughly comparable, since SD-based FCIQMC is generally faster for a given walker number, as discussed in the literature.[9,33] For all walker populations the spin expectation values have been used to confirm convergence to the correct spin state and monitor spin contamination. The deviation was larger for the singlet whose mean spin expectation value was 1.3×10^{-5}, compared to the theoretical 0.

Manganese cluster. Two active spaces have been defined to test the spin penalty approach on the $[Mn_3O_4]^{3+}$ tri-nuclear cluster (Figure 3). A small CAS(9,9) is uti-
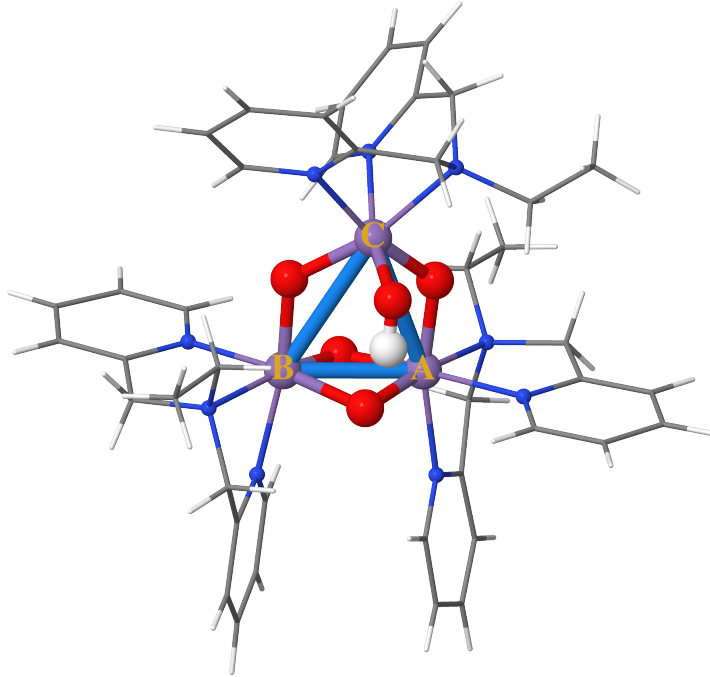

Figure 3: Structure of the $[Mn_3O_4]$ tri-nuclear model system extracted from ref 56. (A), (B) and (C) labels identify the Mn(IV) magnetic centers. Oxygen, nitrogen, carbon and hydrogen atoms are labeled in red, blue, gray and white, respectively.

lized to directly compare to the fully deterministic GUGA-based spin gap.[57,58] A larger CAS(55,38) has been employed to demonstrate the numerical stability of the method in more realistic scenarios. The CAS(9,9) consists of the 9 singly occupied t_{2g} orbitals on

the three magnetic centers. The large active space consists of the fifteen $3\,\mathrm{d}$ orbitals and their 9 electrons, the twelve doubly occupied $2\,\mathrm{p}$ orbitals of the bridging oxygen atoms, the ten doubly occupied peripheral lone-pair orbitals pointing at the metal sites, and two doubly occupied orbitals of the $-\mathrm{OH}$ group, of σ and π character. A similar active space has been previously chosen for a similar $[\mathrm{Mn_3O_4}]$ cluster.[35,59]

Through experimental investigation, Armstrong showed that the ground state of this system is a $\Gamma^{(3/2)}$ spin state.[56] The too small CASSCF(9,9) erroneously predicts a $\Gamma^{(9/2)}$ ground state. Nonetheless, this small model calculation represents an interesting test case to explore the applicability of the spin penalty strategy. The larger CAS(55,38) describes qualitatively well the spin-state ordering, with a $S = \frac{3}{2}$ ground state and a $S = \frac{1}{2}$ state at slightly higher energy, in line with Armstrong's findings.

In Figure 4, we show the convergence behavior of the FCIQMC dynamics for different J, applied to the CAS(9,9) wave function. For FCIQMC dynamics with $J = 0\,E_\mathrm{h}$ or
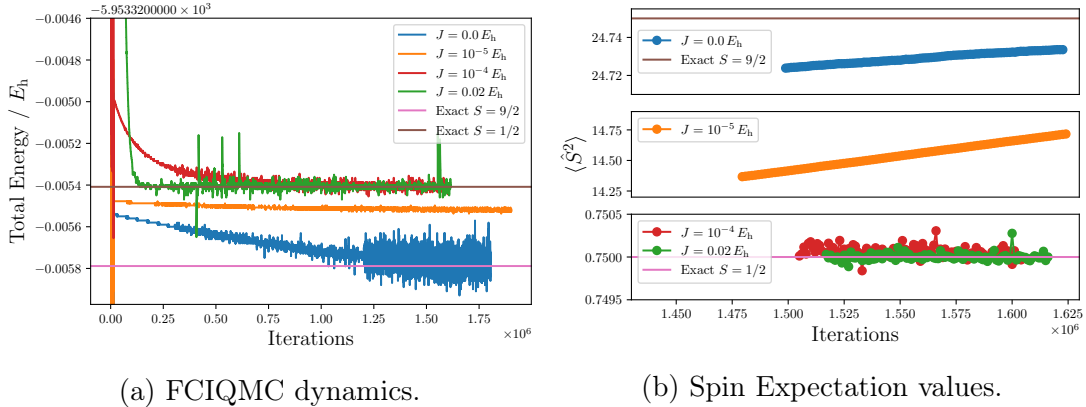

(a) FCIQMC dynamics.

(b) Spin Expectation values.

Figure 4: (a) FCIQMC dynamics varying the amount of spin penalty. The projected energy shifted by the $J \cdot S(S+1)$ value is reported, where S is the *expected* spin value. (b) Spin expectation values calculated from RDMs are shown. All simulations used 5×10^4 walkers.

too small spin penalties ($J = 1 \times 10^{-5}\,E_\mathrm{h}$) the flipping point is not reached, and the FCIQMC dynamics converges to the high-spin state ($S = \frac{9}{2}$), which is the ground state for the small CAS(9,9) model active space. For J values above the flipping point, the low-spin state wave function is obtained. These results are confirmed by the total spin expectation value (Figure 4b). Speed of convergence increases for larger penalty values, and a large range of J values ($1 \times 10^{-4}\,E_\mathrm{h} \leq J \leq 2 \times 10^{-2}\,E_\mathrm{h}$) exists that provides

stable and fast converging FCIQMC dynamics. Too large J values ($> 1 \times 10^{-1} E_\mathrm{h}$) lead to convergence problems.

For the CAS(55,38) model active space the competing doublet ($S = \frac{1}{2}$) and quartet ($S = \frac{3}{2}$) spin state wave functions have been optimized. GUGA-FCIQMC has been utilized as reference. Three choices of J were used that permitted the characterization of the doublet spin state, namely $J = 1 \times 10^{-2} E_\mathrm{h}$, $1 \times 10^{-3} E_\mathrm{h}$, and $1 \times 10^{-4} E_\mathrm{h}$. Figure 5 shows the energetics for the $S = \frac{1}{2}$ and $S = \frac{3}{2}$ states, as a function of the walker population. We notice that all dynamics are stable and fast converging. The choice of the large
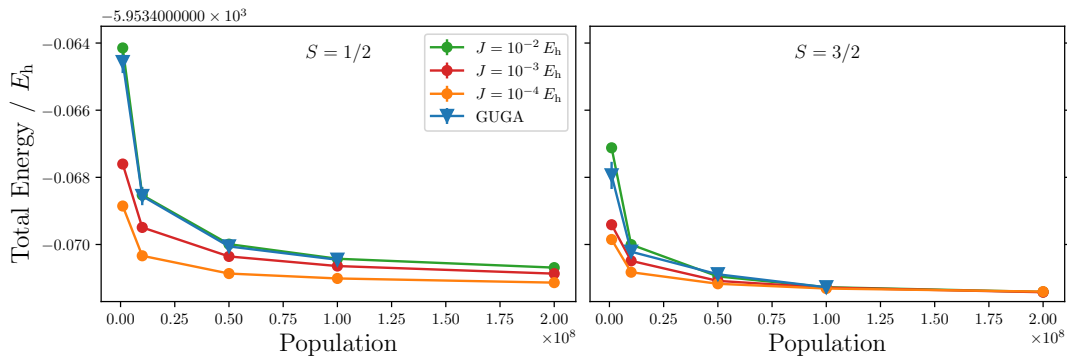

Figure 5: CAS(55,38) total energies, obtained as expectation values from one- and two-body RDMs, for the $S = \frac{1}{2}$ (left) and $S = \frac{3}{2}$ (right) spin states as a function of the walker population. The lower energies for smaller J values are not to be interpreted as a faster convergence with respect to walker number. They are a consequence of the admixing of the targeted spin state with higher spin states (details in the main text).

parameter, $J = 1 \times 10^{-2} E_\mathrm{h}$, results in a nearly exact matching of the spin-purified total energy with the one obtained from the spin-adapted GUGA-FCIQMC approach, at the same walker population.

Lower J values result in lower total energies for low walker populations. The lower energies for smaller J values, are not to be interpreted as a faster convergence of the spin penalty approach for lower J. Instead, considering that the spin expectation value for the smaller $J = 1 \times 10^{-3} E_\mathrm{h}$ is higher than the expected value (Figure 6) we are brought to the conclusion that the unconverged wave function (low population) is in a broken-symmetry state, that results from the mixture of the target spin state ($\Gamma^{(1/2)}$) and the higher spin states (for example $\Gamma^{(3/2)}$). Admixing the higher spin states artificially lowers the total energy. For larger walker populations and for larger J, the spin expectation value
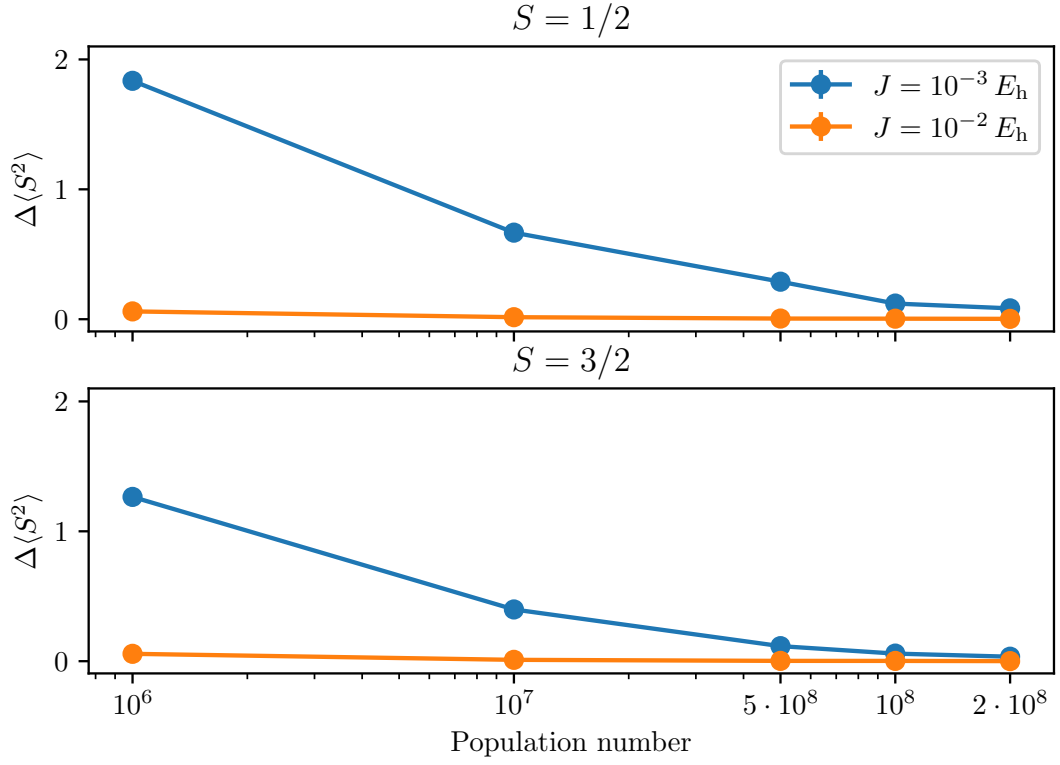
Figure 6: Spin contamination ($\Delta\langle\hat{S}^2\rangle = \langle\hat{S}^2\rangle - S(S+1)$) in the CAS(55,38) for different J and population numbers. The spin $\langle\hat{S}^2\rangle$ was calculated from RDMs. While the larger $J = 1 \times 10^{-2}\,E_{\mathrm{h}}$ value provides dynamics with nearly exact spin expectation values for any chosen walker population, the smaller $J = 1 \times 10^{-3}\,E_{\mathrm{h}}$ calculations converge to the correct spin expectation value slower and only for larger populations.

gets closer to the targeted value, eliminating any spin contamination from the optimized wave function.

It is worth noting that the 38 active orbitals have been localized and reordered to reach maximum compression of the GUGA wave function (see ref 33–35 for details). In Figure 11 of ref 34 we have shown that GUGA-FCIQMC converges faster than the Slater determinant FCIQMC counterpart, when using a tailored (in this case localized) MO basis. Thus, we expect that the chosen one-electron basis utilized for the CAS(55,38) calculation in general favors the GUGA-FCIQMC approach. However, we observe very similar convergence of the GUGA and the Slater determinant based spin penalty approaches (for $J = 1 \times 10^{-2} E_\mathrm{h}$). Moreover, it is interesting to notice that for an equivalent wall-clock time, the spin penalty approach can be run at higher walker population (2×10^8 walkers in the spin penalty method versus 1×10^8 walkers in GUGA) and reaches an overall lower total energy. These results suggest an overall better performance of the spin-purification approach. However, the GUGA strategy has two crucial advantages that we have documented in recent works:[32–35] (a) within GUGA the space of the leading electronic configurations (CSFs) can be greatly reduced and directly connected to physical concepts, and (b) the GUGA CI Hamiltonian matrix has a unique quasi-block-diagonal structure, allowing for unprecedented *state-specific* optimizations of ground- and/or excited-states.

As a final remark, we observe that the spin-penalty strategy enables the combined S- and M_S-adaptation. This scheme is thus more flexible than the GUGA S-adaptation, and allows for the treatment of anisotropic Hamiltonians. In this respect, one pays simplicity and universality for lower dimensionality when going from the M_S-adapted space to the S-adapted one. Moreover, while stochastically sampled higher order density matrices are already available within the SD-based FCIQMC approach, allowing for multi-reference second order perturbation theory (PT2) methods,[60,61] GUGA-FCIQMC three- and four-body density matrices are not available, preventing for the moment GUGA-based PT2 strategies. Additionally, it is possible to envision spin-pure similarity-transformed FCIQMC calculations based on transcorrelated methods[62–69] using the current spin penalty approach, while technical difficulties exist within the GUGA scheme,

because of the presence of three-body interactions in the transcorrelated Hamiltonian.

In conclusion, we have demonstrated that spin purification based on a first-order spin penalty can be efficiently applied to the Slater determinant based FCIQMC algorithm. We have also explained the origin of an optimal J value, and that too large J parameters are to be avoided as they result in mixing of same-spin states, hard to resolve within FCIQMC. The method was successfully applied to calculate the $^1\Delta_g \leftarrow {}^3\Sigma_g$ transition in the O_2 dimer and the $\Gamma^{(1/2)} \leftarrow \Gamma^{(3/2)}$ (and $\Gamma^{(9/2)}$) transition in a $[Mn_3O_4]^{3+}$ tri-nuclear cluster model. The range of applicability of the spin penalty FCIQMC approach is very broad, including the coupling of large active space Stochastic-CASSCF and Stochastic-GASSCF wave functions to methods capable to recover dynamic correlation outside the active space, such as MC-PDFT,[70,71] and crucially methods that require high-order interactions (for example in the form of three- and four-body RDMs) such as PT2 and similarity-transformed techniques. A large range of chemical systems and models for solid state materials can be investigated, including ferromagnetic superconductors of practical interest, such as UGe_2[72] and $URhGe$.[73] The method can also be extended to model Hamiltonians, such as the Hubbard model, often used to investigate spin interactions in strongly correlated materials. By this approach we are able to tackle anisotropic Hamiltonians and, as *spin-resolved* density matrices are available, spin-dependent properties, such as the hyperfine coupling tensors (pivotal in characterizing spin interactions in poly-nuclear transition metal clusters), are within reach. These aspects will be the subject of future work.

Acknowledgement

References

(1) Sharma, S.; Chan, G. K.-L. Spin-adapted density matrix renormalization group algorithms for quantum chemistry. *J. Chem. Phys.* **2012**, *136*, 124121–124137.

(2) Ma, D.; Li Manni, G.; Gagliardi, L. The generalized active space concept in multiconfigurational self-consistent field methods. *J. Chem. Phys.* **2011**, *135*, 044128–044138.

(3) Li Manni, G.; Ma, D.; Aquilante, F.; Olsen, J.; Gagliardi, L. SplitGAS Method for Strong Correlation and the Challenging Case of Cr_2. *J. Chem. Theory Comput.* **2013**, *9*, 3375–3384.

(4) Li, Z.; Chan, G. K.-L. Spin-Projected Matrix Product States: Versatile Tool for Strongly Correlated Systems. *J. Chem. Theory Comput.* **2017**, *13*, 2681–2695.

(5) Qiu, Y.; Henderson, T. M.; Zhao, J.; Scuseria, G. E. Projected coupled cluster theory. *J. Chem. Phys.* **2017**, *147*, 064111–064126.

(6) Tsuchimochi, T.; Ten-no, S. L. Extending spin-symmetry projected coupled-cluster to large model spaces using an iterative null-space projection technique. *J. Comput. Chem.* **2019**, *40*, 265–278.

(7) Shepard, R.; Gidofalvi, G.; Brozell, S. R. The multifacet graphically contracted function method. I. Formulation and implementation. *J. Chem. Phys.* **2014**, *141*, 064105–064130.

(8) Gidofalvi, G.; Brozell, S. R.; Shepard, R. Wave function analysis with Shavitt graph density in the graphically contracted function method. *Theor. Chem. Acc.* **2014**, *133*, 1512–1522.

(9) Dobrautz, W.; Smart, S. D.; Alavi, A. Efficient formulation of full configuration interaction quantum Monte Carlo in a spin eigenbasis via the graphical unitary group approach. *J. Chem. Phys.* **2019**, *151*, 094104–094136.

(10) Guther, K.; Anderson, R. J.; Blunt, N. S.; Bogdanov, N. A.; Cleland, D.; Dattani, N.; Dobrautz, W.; Ghanem, K.; Jeszenszki, P.; Liebermann, N. et al. NECI: N-Electron Configuration Interaction with an emphasis on state-of-the-art stochastic methods. *J. Chem. Phys.* **2020**, *153*, 034107–034131.

(11) Zhang, N.; Liu, W.; Hoffmann, M. R. Iterative Configuration Interaction with Selection. *J. Chem. Theory Comput.* **2020**, *16*, 2296–2316.

(12) Chilkuri, V. G.; Neese, F. Comparison of many-particle representations for selected-CI I: A tree based approach. *J. Comput. Chem.* **2021**, *42*, 982–1005.

(13) Chilkuri, V. G.; Neese, F. Comparison of Many-Particle Representations for Selected Configuration Interaction: II. Numerical Benchmark Calculations. *J. Chem. Theory Comput.* **2021**, *17*, 2868–2885.

(14) Mato, J.; Gordon, M. S. A general spin-complete spin-flip configuration interaction method. *Phys. Chem. Chem. Phys.* **2018**, *20*, 2615–2626.

(15) Paldus, J. Matrix elements of unitary group generators in many-fermion correlation problem. I. tensorial approaches. *J. Math. Chem.* **2021**, *59*, 1–36.

(16) Paldus, J. Matrix elements of unitary group generators in many-fermion correlation problem. II. Graphical methods of spin algebras. *J. Math. Chem.* **2021**, *59*, 37–71.

(17) Paldus, J. Group theoretical approach to the configuration interaction and perturbation theory calculations for atomic and molecular systems. *J. Chem. Phys.* **1974**, *61*, 5321–5330.

(18) Paldus, J. A pattern calculus for the unitary group approach to the electronic correlation problem. *Int. J. Quantum Chem.* **1975**, *9*, 165–174.

(19) Paldus, J. Unitary-group approach to the many-electron correlation problem: Relation of Gelfand and Weyl tableau formulations. *Phys. Rev. A* **1976**, *14*, 1620–1625.

(20) Paldus, J. *Electrons in Finite and Infinite Structures*; Springer US, 1977; pp 411–429.

(21) Shavitt, I. Graph theoretical concepts for the unitary group approach to the many-electron correlation problem. *Int. J. Quantum Chem.* **1977**, *12*, 131–148.

(22) Shavitt, I. Matrix Element Evaluation in the Unitary Group Approach to the Electron Correlation Problem. *Int. J. Quantum Chem.* **1978**, *14 S12*, 5–32.

(23) Paldus, J.; Boyle, M. J. Unitary Group Approach to the Many-Electron Correlation Problem via Graphical Methods of Spin Algebras. *Phys. Scr.* **1980**, *21*, 295–311.

(24) Shavitt, I. In *The Unitary Group for the Evaluation of Electronic Energy Matrix Elements*; Hinze, J., Ed.; Springer: Berlin, Heidelberg, 1981; pp 51–99.

(25) Paldus, J. In *Unitary Group Approach to Many-Electron Correlation Problem*; Hinze, J., Ed.; Springer: Berlin, Heidelberg, 1981; pp 1–50.

(26) Paldus, J. In *Theoretical Chemistry Advances and Perspectives*; Eyring, H., Ed.; Academic Press: New York, 1976; Vol. 2.

(27) Booth, G. H.; Thom, A. J. W.; Alavi, A. Fermion Monte Carlo without fixed nodes: A game of life, death, and annihilation in Slater determinant space. *J. Chem. Phys.* **2009**, *131*, 054106–054115.

(28) Overy, C.; Booth, G. H.; Blunt, N. S.; Shepherd, J. J.; Cleland, D.; Alavi, A. Unbiased Reduced Density Matrices and Electronic Properties from Full Configuration Interaction Quantum Monte Carlo. *J. Chem. Phys.* **2014**, *141*, 244117–244127.

(29) Blunt, N. S.; Smart, S. D.; Booth, G. H.; Alavi, A. An Excited-State Approach Within Full Configuration Interaction Quantum Monte Carlo. *J. Chem. Phys.* **2015**, *143*, 134117–134125.

(30) Blunt, N. S.; Booth, G. H.; Alavi, A. Density matrices in full configuration interaction quantum Monte Carlo: Excited states, transition dipole moments, and parallel distribution. *J. Chem. Phys.* **2017**, *146*, 244105–244116.

(31) Li Manni, G.; Smart, S. D.; Alavi, A. Combining the Complete Active Space Self-Consistent Field Method and the Full Configuration Interaction Quantum

Monte Carlo within a Super-CI Framework, with Application to Challenging Metal-Porphyrins. *J. Chem. Theory Comput.* **2016**, *12*, 1245–1258.

(32) Dobrautz, W.; Weser, O.; Bogdanov, N. A.; Alavi, A.; Li Manni, G. Spin-Pure Stochastic-CASSCF via GUGA-FCIQMC Applied to Iron–Sulfur Clusters. *J. Chem. Theory Comput.* **2021**, *17*, 5684–5703.

(33) Li Manni, G.; Dobrautz, W.; Alavi, A. Compression of Spin-Adapted Multiconfigurational Wave Functions in Exchange-Coupled Polynuclear Spin Systems. *J. Chem. Theory Comput.* **2020**, *16*, 2202–2215.

(34) Li Manni, G.; Dobrautz, W.; Bogdanov, N. A.; Guther, K.; Alavi, A. Resolution of Low-Energy States in Spin-Exchange Transition-Metal Clusters: Case Study of Singlet States in [Fe(III)$_4$S$_4$] Cubanes. *J. Phys. Chem. A* **2021**, *125*, 4727–4740.

(35) Li Manni, G. Modeling magnetic interactions in high-valent trinuclear [Mn$_3$(IV)O$_4$]$_4{}^+$ complexes through highly compressed multi-configurational wave functions. *Phys. Chem. Chem. Phys.* **2021**, *23*, 19766–19780.

(36) Dobrautz, W.; Katukuri, V. M.; Bogdanov, N. A.; Kats, D.; Li Manni, G.; Alavi, A. Combined unitary and symmetric group approach applied to low-dimensional spin systems. *ArXiv* **2021**, arXiv:2112.09594.

(37) Holmes, A. A.; Tubman, N. M.; Umrigar, C. J. Heat-Bath Configuration Interaction: An Efficient Selected Configuration Interaction Algorithm Inspired by Heat-Bath Sampling. *J. Chem. Theory Comput.* **2016**, *12*, 3674–3680.

(38) Tubman, N. M.; Lee, J.; Takeshita, T. Y.; Head-Gordon, M.; Whaley, K. B. A deterministic alternative to the full configuration interaction quantum Monte Carlo method. *J. Chem. Phys.* **2016**, *145*, 044112–044118.

(39) Garniron, Y.; Scemama, A.; Loos, P.-F.; Caffarel, M. Hybrid stochastic-deterministic calculation of the second-order perturbative contribution of multireference perturbation theory. *J. Chem. Phys.* **2017**, *147*, 034101–034109.

(40) Loos, P.-F.; Scemama, A.; Blondel, A.; Garniron, Y.; Caffarel, M.; Jacquemin, D. A Mountaineering Strategy to Excited States: Highly Accurate Reference Energies and Benchmarks. *J. Chem. Theory Comput.* **2018**, *14*, 4360–4379.

(41) Garniron, Y.; Scemama, A.; Giner, E.; Caffarel, M.; Loos, P.-F. Selected configuration interaction dressed by perturbation. *J. Chem. Phys.* **2018**, *149*, 064103–064108.

(42) Scemama, A.; Benali, A.; Jacquemin, D.; Caffarel, M.; Loos, P.-F. Excitation energies from diffusion Monte Carlo using selected configuration interaction nodes. *J. Chem. Phys.* **2018**, *149*, 034108–034115.

(43) Liu, W.; Hoffmann, M. R. iCI: Iterative CI toward full CI. *J. Chem. Theory Comput.* **2016**, *12*, 1169–1178.

(44) Liu, W.; Hoffmann, M. R. SDS: the static–dynamic–static framework for strongly correlated electrons. *Theor. Chem. Acc.* **2014**, *133*, 1481–1492.

(45) Ma, D.; Li Manni, G.; Olsen, J.; Gagliardi, L. Second-Order Perturbation Theory for Generalized Active Space Self-Consistent-Field Wave Functions. *J. Chem. Theory Comput.* **2016**, *12*, 3208–3213.

(46) Weser, O.; Freitag, L.; Guther, K.; Alavi, A.; Li Manni, G. Chemical insights into the electronic structure of Fe(II) porphyrin using FCIQMC, DMRG, and generalized active spaces. *Int. J. Quantum Chem.* **2021**, *121*, e26454–26467.

(47) Weser, O.; Guther, K.; Ghanem, K.; Li Manni, G. Stochastic Generalized Active Space Self-Consistent Field: Theory and Application. *J. Chem. Theory Comput.* **2022**, *18*, 251–272.

(48) Odoh, S. O.; Li Manni, G.; Carlson, R. K.; Truhlar, D. G.; Gagliardi, L. Separated-Pair Approximation and Separated-Pair Pair-Density Functional Theory. *Chem. Sci.* **2016**, *7*, 2399–2413.

(49) Booth, G. H.; Cleland, D. M.; Thom, A. J. W.; Alavi, A. Breaking the Carbon Dimer. *J. Chem. Phys.* **2011**, *135*, 084104–084117.

(50) Fales, B. S.; Hohenstein, E. G.; Levine, B. G. Robust and Efficient Spin Purification for Determinantal Configuration Interaction. *J. Chem. Theory Comput.* **2017**, *13*, 4162–4172.

(51) Marti, K. H.; Ondík, I. M.; Moritz, G.; Reiher, M. Density matrix renormalization group calculations on relative energies of transition metal complexes and clusters. *J. Chem. Phys.* **2008**, *128*, 014104–014116.

(52) Li, Z.; Chan, G. K.-L. Hilbert space renormalization for the many-electron problem. *J. Chem. Phys.* **2016**, *144*, 084103–084125.

(53) Helgaker, T.; Jørgensen, P.; Olsen, J. *Molecular Electronic-Structure Theory*; John Wiley & Sons, Ltd, 2000.

(54) Widmark, P.-O.; Malmqvist, P.-Å.; Roos, B. O. Density Matrix Averaged Atomic Natural Orbital (ANO) Basis Sets for Correlated Molecular Wave Functions. *Theor. Chem. Acc.* **1990**, *77*, 291–306.

(55) Roos, B. O.; Malmqvist, P.-Å. Relativistic Quantum Chemistry: The Multiconfigurational Approach. *Phys. Chem. Chem. Phys.* **2004**, *6*, 2919–2927.

(56) Pal, S.; Chan, M. K.; Armstrong, W. H. Ground spin state variability in manganese oxo aggregates. Demonstration of an $S = 3/2$ ground state for $[Mn_3O_4(OH)(bpea)_3](ClO_4)_3$. *J. Am. Chem. Soc.* **1992**, *114*, 6398–6406.

(57) Aquilante, F.; Autschbach, J.; Carlson, R. K.; Chibotaru, L. F.; Delcey, M. G.; De Vico, L.; Fdez. Galván, I.; Ferré, N.; Frutos, L. M.; Gagliardi, L. et al. Molcas 8: New Capabilities for Multiconfigurational Quantum Chemical Calculations Across the Periodic Table. *J. Comput. Chem.* **2016**, *37*, 506–541.

(58) Fdez. Galván, I.; Vacher, M.; Alavi, A.; Angeli, C.; Aquilante, F.; Autschbach, J.; Bao, J. J.; Bokarev, S. I.; Bogdanov, N. A.; Carlson, R. K. et al. OpenMolcas: From Source Code to Insight. *J. Chem. Theory Comput.* **2019**, *15*, 5925–5964.

(59) Sarneski, J. E.; Thorp, H. H.; Brudvig, G. W.; Crabtree, R. H.; Schulte, G. K. Assembly of high-valent oxomanganese clusters in aqueous solution. Redox equilibrium of water-stable $Mn_3O_4^{4+}$ and $Mn_2O_2^{3+}$ complexes. *J. Am. Chem. Soc.* **1990**, *112*, 7255–7260.

(60) Anderson, R. J.; Shiozaki, T.; Booth, G. H. Efficient and stochastic multireference perturbation theory for large active spaces within a full configuration interaction quantum Monte Carlo framework. *J. Chem. Phys.* **2020**, *152*, 054101–054116.

(61) Halson, J. J.; Anderson, R. J.; Booth, G. H. Improved stochastic multireference perturbation theory for correlated systems with large active spaces. *Mol. Phys.* **2020**, *118*, e1802072–1802084.

(62) Boys, S. F.; Handy, N. C.; Linnett, J. W. The determination of energies and wavefunctions with full electronic correlation. *Proc. Roy. Soc. A* **1969**, *310*, 43–61.

(63) Boys, S. F.; Handy, N. C.; Linnett, J. W. A calculation for the energies and wavefunctions for states of neon with full electronic correlation accuracy. *Proc. Roy. Soc. A* **1969**, *310*, 63–78.

(64) Boys, S. F.; Handy, N. C.; Linnett, J. W. A first solution, for LiH, of a molecular transcorrelated wave equation by means of restricted numerical integration. *Proc. Roy. Soc. A* **1969**, *311*, 309–329.

(65) Handy, N. C. Energies and Expectation Values for Be by the Transcorrelated Method. *J. Chem. Phys.* **1969**, *51*, 3205–3212.

(66) Handy, N. The transcorrelated method for accurate correlation energies using gaussian-type functions: examples on He, H_2, LiH and H_2O. *Mol. Phys.* **1972**, *23*, 1–27.

(67) Luo, H.; Alavi, A. Combining the Transcorrelated Method with Full Configuration Interaction Quantum Monte Carlo: Application to the Homogeneous Electron Gas. *J. Chem. Theory Comput.* **2018**, *14*, 1403–1411.

(68) Cohen, A. J.; Luo, H.; Guther, K.; Dobrautz, W.; Tew, D. P.; Alavi, A. Similarity transformation of the electronic Schrödinger equation via Jastrow factorization. *J. Chem. Phys.* **2019**, *151*, 061101–061105.

(69) Guther, K.; Cohen, A. J.; Luo, H.; Alavi, A. Binding curve of the beryllium dimer using similarity-transformed FCIQMC: Spectroscopic accuracy with triple-zeta basis sets. *J. Chem. Phys.* **2021**, *155*, 011102–011109.

(70) Li Manni, G.; Carlson, R. K.; Luo, S.; Ma, D.; Olsen, J.; Truhlar, D. G.; Gagliardi, L. Multiconfiguration Pair-Density Functional Theory. *J. Chem. Theory Comput.* **2014**, *10*, 3669–3680.

(71) Gagliardi, L.; Truhlar, D. G.; Li Manni, G.; Carlson, R. K.; Hoyer, C. E.; Bao, J. L. Multiconfiguration Pair-Density Functional Theory: A New Way to Treat Strongly Correlated Systems. *Acc. Chem. Res.* **2017**, *50*, 66–73.

(72) Saxena, S.; Agarwal, P.; Ahilan, K.; Grosche, F. M.; Haselwimmer, R. K. W.; Steiner, M. J.; Pugh, E. Superconductivity on the border of itinerant-electron ferromagnetism in UGe2. *Nature* **2000**, *406*, 587–592.

(73) Aoki, D.; Huxley, A.; Ressouche, E.; Braithwaite, D.; Flouquet, J.; Brison, J.-P.; Lhotel, E.; Paulsen, C. Coexistence of superconductivity and ferromagnetism in URhGe. *Nature* **2001**, *413*, 613–616.